Evaluation of Bremsstrahlung Cross Sections at the High-Frequency Limit

U. FANO, H. W. KOCH, AND J. W. MOTZ
National Bureau of Standards, Washington, D. C.

(Received August 4, 1958)

Recent experimental values for the bremsstrahlung cross section near the high-frequency limit with electron energies from 0.05 to 15 Mev and with target atomic numbers from 13 to 79 are compared with theoretical estimates. Calculations made to lowest order in $Z/137$ show large differences with the experimental results for large Z. Improved estimates, derived by detailed balancing arguments from more accurate photoelectric cross sections, agree reasonably well with the experimental results throughout the indicated range of electron energies and atomic numbers.

THEORETICAL estimates of the bremsstrahlung cross section near the high-frequency limit have not been available for comparison with recent measurements.[1–4] In particular, Born-approximation calculations[5] break down completely at the high-frequency limit. The Bethe-Maximon method[6] does not apply, and the exact Sommerfeld calculations[7] are only valid for nonrelativistic electron energies (less than 10 kev). Only estimated corrections to the Born-approximation theory have been suggested.[8]

A Sauter approximation method has been recently developed[9] for calculating the cross section at the high-frequency limit. The method applies to an outgoing electron with velocity near to zero and involves an expansion in powers of $Z/137\beta_0$ and $Z/137$ instead of $Z/137\beta$ as used in the Born approximation. (β_0 and β are, respectively, the incoming and outgoing electron velocities divided by the velocity of light.) In the Sauter approximation, detailed-balancing arguments can be used to relate this cross section to the photoelectric cross section for the K shell. Inspection of experimental data shows that for high-Z targets, the Sauter approximation is inadequate both for bremsstrahlung (see Figs. 1–5) and photoelectric cross section calculations (see reference 5, p. 210, Tables II and III). However the connection between the bremsstrahlung and photoelectric processes is not restricted to the Sauter approximation; on the contrary, one can relate the more accurate experimental and theoretical results available for the photoeffect to bremsstrahlung calculations.

The detailed balancing connection between the photoelectric and bremsstrahlung cross section is based on the following arguments. (a) Emission of bremsstrahlung near the high-frequency limit may leave the electron in states with alternative sets of quantum numbers l and j (although the values $l=0$, $j=\frac{1}{2}$ are most likely). (b) The wave function of a bound atomic electron with quantum numbers n, l, j, goes over at the limit $n\rightarrow\infty$ into a free-electron wave function with the same quantum numbers l and j. This limit is approached rapidly by the values of the wave function near the nucleus, which alone are relevant, at relativistic energies, to the photoeffect or to the emission of x-rays at the high-frequency limit.[10] (c) For the comparison of properties of highly excited bound states with quantum numbers n, l, j, with those of free particle states of the same l and j, each discrete bound state corresponds to a band of free particle states whose width equals the energy separation of successive bound states $E_{nlj}-E_{n-1lj}$. (d) Allowance must be made for differences in the density of final states and in the velocities of the incident electron and x-ray for the processes of bremsstrahlung and photoeffect, respectively.

On this basis, the probability that an electron of energy E_0 emits a photon of energy $k=E_0-mc^2$ and is left with zero kinetic energy in a state with quantum numbers l, j, can be related to the cross section σ_{nlj} for absorption of a photon of energy k by $2j+1$ electrons occupying an atomic subshell with quantum numbers nlj. The cross section for bremsstrahlung emission at the high-frequency limit is obtained by summing over all values of l and j and is

$$\left(\frac{d\sigma}{dk}\right)_{k=E_0-mc^2}=\frac{E_0-mc^2}{E_0+mc^2}\left[\sum_{lj}\frac{\sigma_{nlj}}{E_{nlj}-E_{n-1lj}}\right]_{n\rightarrow\infty}. \quad (1)$$

The factor $(E_0-mc^2)/(E_0+mc^2)$, which is equal to $k^2/\beta_0 p_0 E_0 c$ takes into account that (a) the numbers of states available for bremsstrahlung and photoelectron emission are in a ratio k^2/p_0E_0c, and (b) the ratio of the incident beam velocities for bremsstrahlung and photoeffect is β_0.

For high-energy photons and for an electron shell of given n, the photoelectric cross section, $\sigma_{n0\frac{1}{2}}$, of the $s_{\frac{1}{2}}$

[1] J. W. Motz and R. C. Placious, Phys. Rev. **109**, 235 (1958).
[2] J. W. Motz, Phys. Rev. **100**, 1560 (1955).
[3] N. Starfelt and H. W. Koch, Phys. Rev. **102**, 1598 (1956).
[4] Fuller, Hayward, and Koch, Phys. Rev. **109**, 630 (1958).
[5] See, e.g., W. Heitler, *Quantum Theory of Radiation* (Oxford University Press, Oxford, 1956), third edition, pp. 242–247.
[6] H. A. Bethe and L. C. Maximon, Phys. Rev. **93**, 768 (1954).
[7] A. Sommerfeld, *Wellenmechanik* (Frederick Ungar Publishing Company, New York, 1950), Chap. 7.
[8] G. Elwert, Ann. Physik **34**, 178 (1939); E. Guth, Phys. Rev. **59**, 329 (1941). In addition, F. Nagasaka (University of Notre Dame thesis, 1955) and M. V. Mihailovic, Nuovo cimento **9**, 331 (1958), have carried out calculations at the high-frequency limit using Sommerfeld-Maue wave functions; however they do not discuss the significance of these wave functions at $\beta=0$.
[9] U. Fano (to be published).
[10] The screening action of atomic electrons differs in the photoelectric and bremsstrahlung processes, but this difference should be very small near the nucleus.

subshell exceeds greatly the cross section for the other subshells. More specifically, the ratio $\sigma_{nlj}/\sigma_{n0\frac{1}{2}}$ for $l\neq 0$ is generally larger than one at the photoelectric threshold of the nth shell but *decreases rapidly* with increasing photon energy and eventually becomes much smaller than one.[11] Therefore, a first simplification, to be called *simplification A*, can be made by disregarding the terms with $l\neq 0$ of the sum in (1). These terms are actually of higher order in $Z/137\beta_0$ and have therefore been disregarded in the Sauter approximation treatment of reference 9. Another important simplification, to be called *simplification B*, holds in the Sauter approximation and will be utilized in this paper; it consists of replacing the ratio

$$\lim_{n\to\infty}\left[\sigma_{n0\frac{1}{2}}/(E_{n0\frac{1}{2}}-E_{n-10\frac{1}{2}})\right]$$

at the series limit with a ratio appropriate to the K-shell state, namely, $\sigma_{10\frac{1}{2}}/(Z/137)^2mc^2$.

Even though more information is available on the cross section for the photoelectric effect than for bremsstrahlung at the spectral limit, the information is not quite adequate for the evaluation of the right side of (1). Most of the data pertain to the photoeffect in the K shell, i.e., to $n=1$ and $l=0$. Accordingly we shall use Eq. (1) as a guide to indicate what error is incurred by performing the simplifications A and B and we will substitute a better value of the K-shell cross section $\sigma_{10\frac{1}{2}}$ than is provided by the Sauter approximation. The available data on the photoelectric cross sections are discussed by Bethe and Salpeter,[11] p. 381 ff.; by Heitler,[5] p. 207 ff.; and by Grodstein.[12]

As a first evaluation of the bremsstrahlung cross section at the spectral limit, we have taken the Sauter approximation result from reference 9 which is

$$\left(k\frac{d\sigma}{dk}\right)_{k=E_0-mc^2}=4\pi\frac{Z^3}{(137)^2}\left(\frac{e^2}{mc^2}\right)^2\frac{E_0mc^2}{(E_0-mc^2)^2}\beta_0\times\left\{\frac{4}{3}+\frac{E_0(E_0-2mc^2)}{mc^2(E_0+mc^2)}\left[1-\left(\frac{mc^2}{E_0}\right)^2\frac{1}{2\beta_0}\ln\frac{1+\beta_0}{1-\beta_0}\right]\right\}. \quad (2)$$

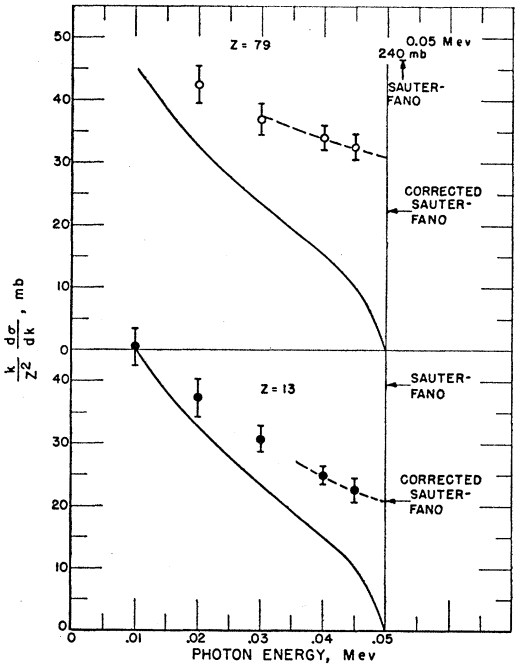

FIG. 1. Dependence of the bremsstrahlung cross section integrated over photon angle on the photon energy for 0.05-Mev electrons. The Born-approximation cross sections are shown by the solid curve, and the experimental values are shown by the open circles for gold and the closed circles for aluminum. The Sauter-Fano and corrected Sauter-Fano arrows indicate the theoretical cross sections at the high-frequency limit which are estimated from the relationship between the bremsstrahlung and photoelectric processes.

TABLE I. Bremsstrahlung cross sections at the high-frequency limit.

Electron kinetic energy (Mev)	Target	$\frac{k}{Z^2}\left[\frac{d\sigma}{dk}\right]_{k=E_0-mc^2}$ (millibarns) Sauter-Fano	Corrected Sauter-Fano	Experimental (extrapolated)
0.05	Al	39.5	21	21±2
	Au	240	23	31±3
0.50	Al	1.64	1.3	1.5±0.6
	Au	9.97	3.4	5.2±2.0
1.00	Al	0.954	0.71	0.6±0.3
	Au	5.80	1.8	1.7±0.7
4.5	Au	4.3	2.0	1.8±0.3
15.1	Al	0.698	0.55	
	Au	4.23	1.77	(1.47±0.44)
	W	3.97	1.66	1.38±0.41

This equation has been derived by applying the simplifications A and B to Eq. (1) and by adopting the Sauter cross section for the photoelectric effect in the K shell. The values obtained in this manner are compared with experimental results in the figures and in Table I, where they are labeled "Sauter-Fano."

It is known[5,11,12] that the Sauter formula greatly overestimates the true values for the photoelectric cross section. Therefore, as a next step of approximation the Sauter value of $\sigma_{10\frac{1}{2}}$ was replaced with more accurate theoretical values as described below for the various energy ranges. The resulting estimates of the bremsstrahlung cross section are called "corrected Sauter-Fano." No attempt was made to correct for the simpli-

[11] See, e.g., H. A. Bethe and E. Salpeter, *Encyclopedia of Physics* (Springer-Verlag, Berlin, 1957), Vol. 35, pp. 393–394.
[12] G. White Grodstein, Natl. Bur. Standards Circ. No. 583 (1957).

fications A and B, whose quantitative influence is discussed in the concluding paragraph.

A detailed comparison between the experimental and theoretical results requires a certain amount of analysis to reduce data from different experiments to a common basis. The comparison is presented in Figs. 1–6. Figures 1–5 show the dependence of the bremsstrahlung cross section integrated over photon angle on the photon energy for given electron energies and target materials. The data for these figures were obtained as follows:

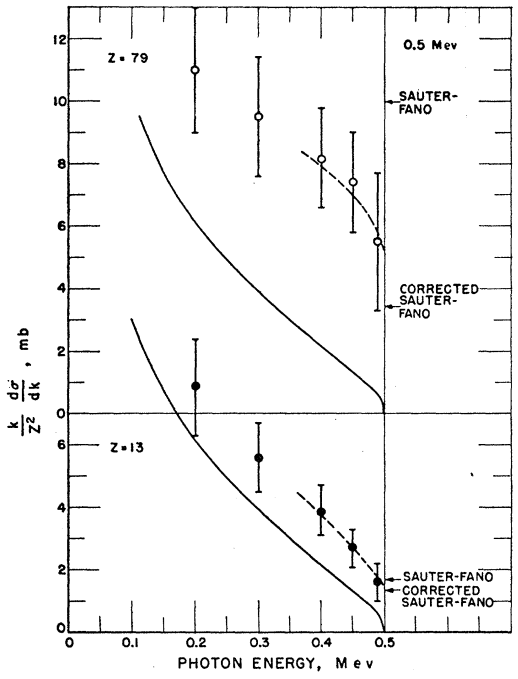

FIG. 2. Dependence of the bremsstrahlung cross section integrated over photon angle on the photon energy for 0.50-Mev electrons. The Born-approximation cross sections are shown by the solid curve, and the experimental values are shown by the open circles for gold and the closed circles for aluminum. The Sauter-Fano and corrected Sauter-Fano arrows indicate the theoretical cross sections at the high-frequency limit which are estimated from the relationship between the bremsstrahlung and photoelectric processes.

(1) In Fig. 1, the experimental results obtained in reference 1 for 0.05-Mev electrons are shown by the open circles for gold and the closed circles for aluminum. The solid curves give the cross sections predicted by the Born-approximation calculations. [See reference 5, Eq. (16), p. 245.] At the high-frequency limit, theoretical values for the cross section are indicated by the arrows. As discussed in the foregoing, the Sauter-Fano values which are obtained from Eq. (2), are only valid if $(Z/137\beta_0)\ll 1$, and are seen in Fig. 1 to be much larger than the experimental values for both aluminum and gold. The corrected Sauter-Fano values are obtained by multiplying the Sauter-Fano values with the ratio of photoelectric cross sections for the K shell that are

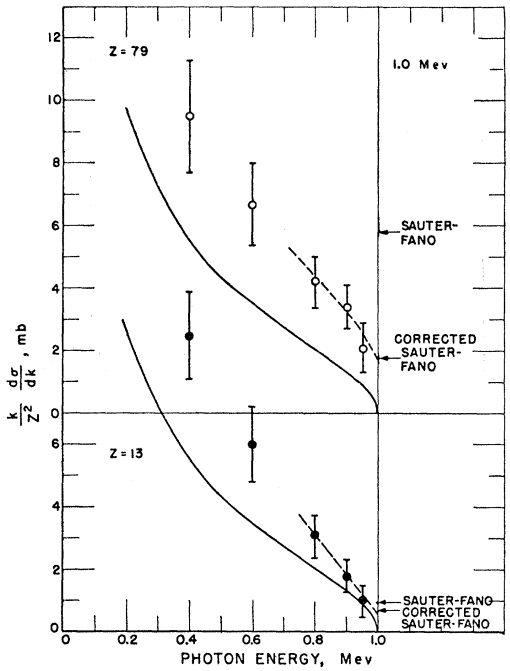

FIG. 3. Dependence of the bremsstrahlung cross section integrated over photon angle on the photon energy for 1.0-Mev electrons. The Born-approximation cross sections are shown by the solid curve, and the experimental values are shown by the open circles for gold and the closed circles for aluminum. The Sauter-Fano and corrected Sauter-Fano arrows indicate the theoretical cross sections at the high-frequency limit which are estimated from the relationship between the bremsstrahlung and photoelectric processes.

derived by "exact" and by Born-type calculations. In the case of aluminum, we used the ratio f as discussed and defined by Eq. (15), p. 208 in reference 5. In the case of gold, we used the same ratio extrapolated according to the procedure of Lewis.[13]

(2) In Figs. 2 and 3, the experimental results obtained in reference 2 for 0.50- and 1.0-Mev electrons, respectively, are shown by the open circles for gold and the closed circles for aluminum. The solid curves give the Born-approximation cross sections. The theoretical cross sections at the high-frequency limit are shown by the arrows and have the same designation as in (1). The corrected Sauter-Fano values were obtained by multiplying the Sauter-Fano values by the ratio of $(\sigma_K)_{\text{Hulme}}$ to $(\sigma_K)_{\text{Sauter}}$, where $(\sigma_K)_{\text{Hulme}}$ is the photoelectric cross section for the K shell derived by Hulme *et al.*[14] with exact relativistic calculations, and $(\sigma_K)_{\text{Sauter}}$ is the same cross section derived in the Sauter approximation. This ratio was evaluated for both aluminum and gold from the Tables II and III in reference 5, p. 210.

(3) In Fig. 4, the experimental results given for 4.5-Mev electrons in reference 3 are shown for a gold

[13] Margaret N. Lewis, Natl. Bur. Standards Rept. 2457 (1953, (unpublished).

[14] Hulme, McDougall, Buckingham, and Fowler, Proc. Roy. Soc (London) 149, 131 (1935).

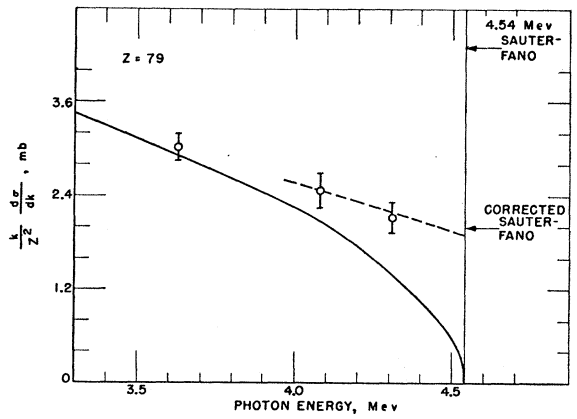

FIG. 4. Dependence of the bremsstrahlung cross section integrated over photon angle on the photon energy for 4.5-Mev electrons. The Born-approximation cross sections are shown by the solid curve. The experimental values are shown by open circles and were inferred for gold from data that was differential in the photon angle. The Sauter-Fano and corrected Sauter-Fano arrows indicate the theoretical cross sections at the high-frequency limit which are estimated from the relationship between the bremsstrahlung and photoelectric processes.

target. In order to obtain a cross section integrated over photon angle, the averaged ratios of the experimental results to the Born-approximation predictions as determined by differential experiments and given in Fig. 11 of reference 3, were applied to the Born-approximation integrated cross sections calculated by means of Eq. (16) of reference 5. The result is shown in Fig. 4 for the energy region close to the high-frequency limit of a 4.5-Mev spectrum. The solid curve is the Born-approximation cross section. The theoretical values at the high-frequency limit are shown by the arrows. The correction factor to the Sauter-Fano value was taken as the ratio of the Nagasaka[15] to the Sauter photoelectric cross section. The Nagasaka cross section was selected because this calculation was performed with the Sommerfeld-Maue wave function for the final state and the exact Dirac wave function for the initial state of the K electron. The calculation agrees with Hulme's exact calculations at $0.69m_0c^2$ and $2.2m_0c^2$ and should be more correct than any other calculation available. See reference 12 for a more detailed discussion.

(4) In Fig. 5, the experimental results obtained in reference 4 are shown for 15.1-Mev electrons and for a 0.010-in. tungsten target.[16] The curves drawn in the

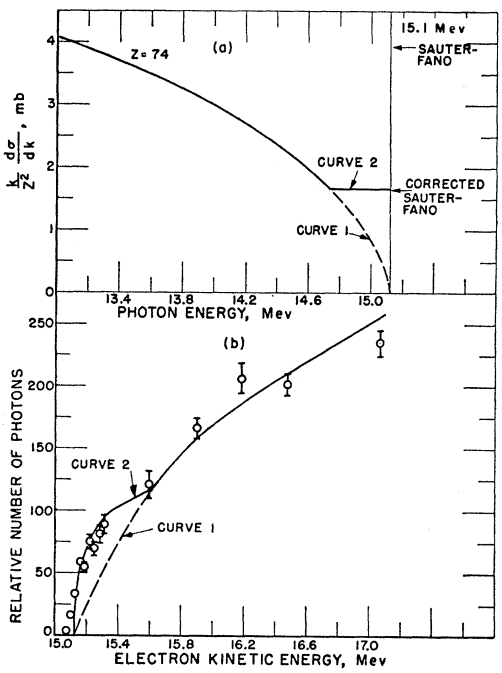

FIG. 5(a). Dependence of the bremsstrahlung cross section integrated over photon angle on the photon energy for 15.12-Mev electrons and for a tungsten target. Curve 1 shows the Born-approximation cross section. The true cross section is assumed to be represented by curve 2 which has the Born shape below 14.74 Mev and has a constant value above 14.74 Mev determined by the corrected Sauter-Fano value. (b) Dependence of the relative number of 15.12-Mev photons produced by electrons with kinetic energies of E_0-mc^2 in a tungsten target whose thickness was 370 kev. Curve 1 is the Born-approximation yield curve corrected for target thickness; curve 2 is the yield curve calculated for spectra similar to curve 2 of (a) corrected for target thickness. The experimental points were obtained from the data of reference 4. The cross-section value at the high-frequency limit as inferred from this comparison for tungsten is $1.65/1.20=1.38(\pm0.41)$ mb. The extrapolated value for gold is $1.47(\pm0.44)$ mb.

upper part of Fig. 5 are (1) the Born-approximation spectrum derived from Eq. (16) of reference 5, and (2) the spectrum shape[17,18] obtained from the corrected

[15] F. G. Nagasaka, thesis University of Notre Dame, 1955 (unpublished); see also reference 12.

[16] Unfortunately, quantitative interpretations of the results in reference 4 are difficult because the targets used were relatively thick and required target corrections; and, more seriously, because the experiment showed evidences for multiple traversals. The only target from which the x-ray angular distribution showed no evidences for multiple traversals was the 0.010-in. tungsten target. Therefore, these data are the only results that are compared with the predictions of this paper. In making this comparison, the experimental points shown in Fig. 4(c) of reference 4 were shifted down by 50 kev. This small modification should provide a more suitable and justified assignment of an energy scale for the present case than the assignment used in reference 4.

[17] The analysis of the experiments at 15 Mev requires an estimate of the cross section for x-ray emission near the limit of the spectrum, because the target thickness was such as to make the incident electron energy inhomogeneous by $\sim$0.4 Mev. This estimate involves an interpolation between the theoretical value expected at the limit and the Born-approximation value corresponding to photon energies 1 or 2 Mev lower than the limit, since the Born-approximation value agrees with experiments rather well at lower photon energies. However, the Sauter approximation utilized in reference 7 provides no firm theoretical basis for the interpolation. Even less guidance is available regarding the variation of the corrective factor $\sigma_K/(\sigma_K)_{\text{Sauter}}$ which we have applied to the Sauter approximation value at the limit.

[18] It is remarkable that the Sauter approximation to the cross section at the limit is in error by a factor greater than two for high-Z targets, whereas the ordinary Born approximation provides a much higher accuracy for energies very close to this limit. This fact may be partially explained by the rapid variation of the minimum value of the nuclear recoil momentum, q, near the limit of the spectrum. In this range we have $q_{\min}\sim mc(mc^2/E)$, where E is the energy of the electron after x-ray emission. It seems plausible that the Born approximation improves rapidly as soon as q becomes smaller than mc, i.e., as soon as the radiation originates outside the immediate vicinity of the nucleus. Another partial

Sauter-Fano value at the limit and from a constant-value interpolation to the Born spectrum. The Sauter-Fano value is also shown. The correction factor was the ratio of the Nagasaka to Sauter photoelectric cross sections. The experiment of reference 4 provides a test of curve (2) of Fig. 5(a) because the shape of the high-frequency end of the spectrum was examined by varying the primary electron kinetic energy and by examining the relative number of photons at 15.12 Mev as a function of electron energy. When the curve (2) is reinterpreted in terms of the photon yield at 15.12 Mev and corrected by the thick-target procedure of Penfold,[19] the result is the predicted curve (2) of Fig. 5(b). Curve (1) is the corrected Born-approximation bremsstrahlung shape. The experimental points at 15.6, 15.9, 16.18, and 17.07 Mev were averaged and normalized to the predicted curves at 16.40 Mev. The experimental data show a cross-section value that is approximately 20% below the curve (2) of Fig. 5(a). The error limits are estimated to be $\pm 15\%$ of this corrected end-point cross section.

Experimental values for the bremsstrahlung cross section at the high-frequency limit were obtained by extrapolation of the experimental points, as shown by the dashed curves in Figs. 1–5. A summary of these values and the corresponding Sauter-Fano and the corrected Sauter-Fano values are shown by the solid and dashed curves, respectively, in Fig. 6.

The corrected Sauter-Fano values are seen to agree reasonably well with the experiments. These estimates should probably be a *little lower* than the true values for the following reasons: (a) The terms with $l \neq 0$ in Eq. (1), which have been disregarded through simplification A, are positive. These terms would probably yield contributions no larger than a very few percent of the corrected Sauter-Fano value for the low-Z targets at all energies and also for the tungsten target

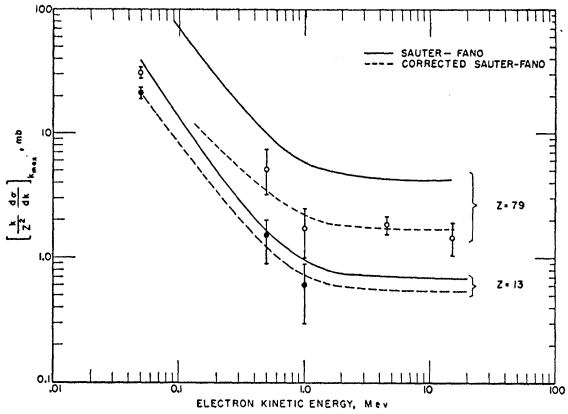

FIG. 6. Dependence of the bremsstrahlung cross section integrated over photon angle at the high-frequency limit on the incident electron kinetic energy. The solid curves (Sauter-Fano) give the values calculated from Eq. (2) and the dashed curves (corrected Sauter-Fano) have been smoothly drawn through the values given in Table I. The experimental values which have been extrapolated to the high-frequency limit from Figs. 1–5 are shown by the open and closed circles for gold and aluminum, respectively.

at 15 Mev. The contribution of terms with $l=1$ should be more substantial for the gold targets at ~ 1 Mev, and very substantial for gold at 0.05 mev. (In this last case the "impact parameter"—defined as the ratio of $\hbar$ to the nuclear recoil momentum—is of the order of the L-shell radius whereas it is smaller than the K-shell radius for all other energies and targets.) (b) The difference in the photoelectric cross sections for the K-shell states and states at the $s_{\frac{1}{2}}$ series limit, which has been disregarded, arises from differences in the magnitude and shape of the wave function near the nucleus. The difference in magnitude increases the cross section at the series limit by a factor $(1+\gamma)/\Gamma(2\gamma+1)$, where $\Gamma(2\gamma+1)$ is the gamma function and $\gamma=(1-Z^2/137^2)^{\frac{1}{2}}$. This factor is approximately 1.24 for gold ($Z=79$). This factor has not been taken into account in the figures because it has little influence as compared to other uncertainties in the discussion. The effect of shape differences in the wave function has not been evaluated.

explanation may be the surmise that the errors introduced by the Born-approximation form of the wave functions before and after the emission of radiation cancel out when both β_0 and β are close to 1. This surmise is suggested by the mathematical form of the "Elwert factor."[5,8]

[19] A. S. Penfold, University of Illinois report (unpublished).